

Atmospheric Measurement Techniques Discussions is the access reviewed discussion forum of *Atmospheric Measurement Techniques*

**Water vapor isotope
measurements by
OA-ICOS**

P. Sturm and A. Knohl

Water vapor $\delta^2\text{H}$ and $\delta^{18}\text{O}$ measurements using off-axis integrated cavity output spectroscopy

P. Sturm and A. Knohl

Institute of Plant Sciences, ETH Zürich, Universitätsstrasse 2, 8092 Zürich, Switzerland

Received: 12 August 2009 – Accepted: 17 August 2009 – Published: 28 August 2009

Correspondence to: P. Sturm (patrick.sturm@ipw.agrl.ethz.ch)

Published by Copernicus Publications on behalf of the European Geosciences Union.

Title Page

Abstract

Introduction

Conclusions

References

Tables

Figures

⏪

⏩

◀

▶

Back

Close

Full Screen / Esc

Printer-friendly Version

Interactive Discussion



Abstract

We present a detailed assessment of a commercially available water vapor isotope analyzer (WVIA, Los Gatos Research, Inc.) for simultaneous in-situ measurements of $\delta^2\text{H}$ and $\delta^{18}\text{O}$ in water vapor. This method, based on off-axis integrated cavity output spectroscopy, is an alternative to the conventional water trap/isotope ratio mass spectrometry (IRMS) techniques. We evaluate the analyzer in terms of precision, memory effects, concentration dependence, temperature sensitivity and long-term stability. A calibration system based on ink jet technology is used to characterize the performance and to calibrate the analyzer. Our results show that the precision at an averaging time of 15 s is 0.16‰ for $\delta^2\text{H}$ and 0.08‰ for $\delta^{18}\text{O}$. The isotope ratios are strongly dependent on the water mixing ratio of the air. Taking into account this concentration dependence as well as the temperature sensitivity of the instrument we obtained a long-term stability of the water isotope measurements of 0.38‰ for $\delta^2\text{H}$ and 0.25‰ for $\delta^{18}\text{O}$. The accuracy of the WVIA was further assessed by comparative measurements using IRMS and a dew point generator indicating a linear response in isotopic composition and H_2O concentrations. The WVIA combined with a calibration system provides accurate high resolution water vapor isotope measurements and opens new possibilities for hydrological and ecological applications.

1 Introduction

The stable isotopes of water are powerful tracers to investigate the hydrological cycle, ecological processes or paleoclimatic archives (Gat, 1996; Farquhar et al., 2007; Barbour, 2007; Andersen et al., 2004). Traditionally, the analysis of the stable isotope composition in water makes use of isotope ratio mass spectrometry (IRMS). Because water can not be directly introduced into the mass spectrometer due to instrumental limitations, isotopic analyses of water involve sample pretreatment. In case of atmospheric water vapor the first step is to trap the water cryogenically or with a molecular

Water vapor isotope measurements by OA-ICOS

P. Sturm and A. Knohl

Title Page

Abstract

Introduction

Conclusions

References

Tables

Figures



Back

Close

Full Screen / Esc

Printer-friendly Version

Interactive Discussion



sieve (Han et al., 2006). The liquid water samples are then either chemically converted into or isotopically equilibrated with a gas (CO_2 , H_2 , CO) suitable for subsequent mass spectrometric analysis. These sample pretreatments are time-consuming and often limit the achievable precision.

5 Recently, laser spectroscopic techniques for water isotope measurements have been developed that achieve similar accuracies as the traditional IRMS methods and overcome some of its disadvantages (Kerstel et al., 1999, 2002; Gianfrani et al., 2003). Water vapor can be directly measured in real time without external sample preparation systems. Furthermore, different isotope ratios ($\delta^2\text{H}$ and $\delta^{18}\text{O}$) can be measured
10 simultaneously and at a high time resolution. The capital and maintenance costs are considerably smaller compared to conventional mass spectrometer techniques. Finally, the lower size and weight as well as the lower power consumption make them potentially field deployable.

In addition to dedicated research instruments several commercial laser based instruments are now available (Lee et al., 2005; Lis et al., 2008; Gupta et al., 2009). In this study, we use the commercially available water vapor isotope analyzer from Los Gatos Research, Inc., which is based on off-axis integrated cavity output spectroscopy (Baer et al., 2002). This instrument provides simultaneous in-situ measurements of $\delta^2\text{H}$ and $\delta^{18}\text{O}$ in water vapor. This opens new possibilities for hydrological and ecological applications. A detailed assessment of the system performance, however, is necessary
20 before such an instrument can be used as a reliable research tool.

A general technical difficulty when measuring water vapor isotopes arises from the nature of the water molecule. The high polarity of water molecules compared to other trace gases results in strong sticking on surfaces. This in turn can lead to slower response times of the instrument and changing isotope ratios due to fractionation effects. Such gas handling issues as well as the high precision and accuracy that is needed to resolve the natural variability in water vapor isotope ratios requires calibration procedures for the instrument. Calibration gases for water vapor isotopes are not commercially available, however. In order to calibrate the system we therefore developed an

Water vapor isotope measurements by OA-ICOS

P. Sturm and A. Knohl

Title Page

Abstract

Introduction

Conclusions

References

Tables

Figures

◀

▶

◀

▶

Back

Close

Full Screen / Esc

Printer-friendly Version

Interactive Discussion



automated calibration device based on ink jet technology (Iannone et al., 2009). Water with a known isotopic signature is injected into a dry air stream, immediately vaporized to prevent any fractionation and then admitted to the analyzer.

Our objective is to present an extensive characterization of the analyzer in terms of precision, memory effects, concentration dependence, temperature sensitivity and long-term stability. The accuracy of the laser spectroscopic measurements is assessed by comparative measurements using isotope ratio mass spectrometry and a dew point generator.

2 Methods

2.1 Water vapor isotope analyzer

We use a commercially available water vapor isotope analyzer (WVIA, DLT-100, Version March 2009) from Los Gatos Research, Inc. This instrument provides simultaneous measurements of $^{18}\text{O}/^{16}\text{O}$ and $^2\text{H}/^1\text{H}$ ratios in ambient water vapor and of water vapor mixing ratios. The analyzer is based on off-axis integrated cavity output spectroscopy (OA-ICOS). A detailed description of this technique is given by Baer et al. (2002) and references therein. In brief, the beam of a near-infrared diode laser is directed off-axis into an optical cavity. The cavity is an absorption cell with highly reflective mirrors (reflectivity ~ 0.9999) at both ends. This results in effective optical path lengths of several kilometers and thus high sensitivities. The wavelength of the laser is tuned over selected absorption lines of the target species and the transmitted laser intensities are recorded by a photodetector. The effective optical path length is determined by regularly switching the laser off and measuring the time necessary for the light to leave the cavity. The measured absorption spectra, combined with measured gas temperatures and pressure in the cell, the measured effective path length and spectroscopic parameters from the HITRAN database (Rothman et al., 2005) are then used to directly determine the mixing ratios of the target species.

Water vapor isotope measurements by OA-ICOS

P. Sturm and A. Knohl

Title Page

Abstract

Introduction

Conclusions

References

Tables

Figures

◀

▶

◀

▶

Back

Close

Full Screen / Esc

Printer-friendly Version

Interactive Discussion



Water vapor isotope measurements by OA-ICOS

P. Sturm and A. Knohl

Title Page

Abstract

Introduction

Conclusions

References

Tables

Figures

◀

▶

◀

▶

Back

Close

Full Screen / Esc

Printer-friendly Version

Interactive Discussion



An external diaphragm vacuum pump (KNF, N920AP.29.18) downstream of the instrument draws air through the measurement cell (Fig. 1). A pressure controller (VSO-EV, Parker) upstream of the cell keeps the cell pressure constant at 50 ± 0.007 hPa. The flow rate through the cell can be varied ($300\text{--}800$ mL min^{-1}) by adjusting the speed of the pump with the integrated potentiometer. All measurements presented here have been performed at a flow rate of 500 mL min^{-1} except as noted otherwise. The measurement cell is about 0.59 m long and has a volume of 830 mL. This corresponds to a cell exchange time of about 3 s for a flow rate of 800 mL min^{-1} STP (standard temperature and pressure) at 50 hPa. To minimize influences of ambient temperature variations the absorption cell is heated to $\sim 47^\circ\text{C}$ (see Sect. 3.4).

The maximal measurement rate is 1 Hz¹. The typical ring-down time, i.e. the cavity decay time of the laser intensity, is 24 μs , which corresponds to an effective optical path length of about 7 km.

The water vapor isotope analyzer measures the mixing ratios of the three water isotopologues $^{16}\text{O}^1\text{H}^{16}\text{O}$, $^{18}\text{O}^1\text{H}^{16}\text{O}$ and $^{16}\text{O}^2\text{H}^{16}\text{O}$ by scanning over three nearby absorption lines with similar line strengths and at a wavelength of ~ 1.389 μm . The measured isotopic ratios are expressed in δ -notation as a deviation from a reference ratio,

$$\delta = \frac{R}{R_{\text{VSMOW}}} - 1 \quad (1)$$

where R is the measured ratio of rare to abundant isotopologue ($^{16}\text{O}^2\text{H}^{16}\text{O}/^{16}\text{O}^1\text{H}^{16}\text{O}$ or $^{18}\text{O}^1\text{H}^{16}\text{O}/^{16}\text{O}^1\text{H}^{16}\text{O}$) and R_{VSMOW} is the respective isotope ratio of the international reference standard for water (Vienna Standard Mean Ocean Water, Gonfiantini, 1978).

The concentration range specified by the manufacturer for isotopic ratio measurements is from about 4000 ppm H_2O mixing ratio to saturation ($\sim 30\,000$ ppm at 24°C). In order to account for applications with very dry conditions, we have extended the range of our tests to H_2O mixing ratios below 4000 ppm.

¹A recently updated version of the instrument software now allows for a maximal measurement rate of 2 Hz (D. Baer, personal communication, 2009).

2.2 Calibration system

In order to continuously access the stability and accuracy of the instrument and also to be able to express the results on an international reference scale, the instrument needs to be calibrated on a regular basis. This poses the question of how water vapor in air with known and constant isotope ratios can be supplied to the instrument. Storing large quantities of moist air in pressurized tanks might only be an option for very low water vapor mixing ratios (Kerstel et al., 2006) as the water vapor partial pressure needs to be below the saturation pressure in order to avoid isotopic fractionation through condensation. Still, other fractionations, e.g. due to wall effects in the tanks, could make it difficult to get accurate standard measurements. Therefore directly adding liquid water to a dry air stream with complete evaporation (to avoid isotopic fractionation) seems to be a more promising approach to generate water vapor standards. One potential implementation would be to use a dew point generator where dry air is bubbled through water held at constant temperature (Wen et al., 2008; Lee et al., 2005; Wang et al., 2009). The water vapor mixing ratio of the saturated air can be determined if water temperature and air pressure are precisely measured. The isotopic ratios of the water vapor can be calculated from the temperature dependent equilibrium fractionation between liquid water and water vapor. An additional challenge, however, is that the source water will become more and more enriched in the heavy isotopes as the water evaporates. The Rayleigh distillation model can be used to determine the enrichment of the source water provided initial and residual water mass in the dew point generator can be accurately measured.

Another alternative for calibration measurements is a liquid autosampler as it is often deployed in IRMS or for liquid water laser spectroscopic analyzers (Lis et al., 2008; Brand et al., 2009). Discrete sub-microliter water samples are injected through a septum in the autosampler and transferred as vapor to the analyzer. A more continuous generation of water vapor can be achieved by using a syringe pump which provides a continuous water flow to an evaporation flask (Wen et al., 2008). Another possibility

Water vapor isotope measurements by OA-ICOS

P. Sturm and A. Knohl

Title Page

Abstract

Introduction

Conclusions

References

Tables

Figures



Back

Close

Full Screen / Esc

Printer-friendly Version

Interactive Discussion



to produce moist air with known isotopic signature is to use a nebulizer or an injector which drips water droplets into a dry air stream.

Our approach to calibrate the instrument is to use a piezo-injector (Iannone et al., 2009). It consists of a dispenser head (Microdrop Technologies GmbH, MD-K-130) and the drive electronics (MD-E-201). The functional principle of this dispensing system is based on piezoelectric ink jet printing technology. A glass capillary is set under pressure by applying short electrical pulses to a piezo actuator. This induces a shock-wave into the fluid contained in the capillary and causes a droplet to be emitted from the nozzle. The inner nozzle diameter of our injector is 50 μm and determines the water droplet diameter of 65 μm , corresponding to a droplet volume of 144 pL. The maximal drop rate is 2000 Hz. The drop rate is controlled via an external trigger signal, which is generated by a data acquisition board (National Instruments, PCI-6010).

A schematic diagram of the gas handling setup for the calibration and sampling system is shown in Fig. 1. For calibration measurements dry air is drawn from a tank of pressurized air and first passes a desiccant tube (“mop-up” dryer) filled with magnesium perchlorate to remove any residual moisture. The air is then flushed into the dripping device, which is a custom made glass flask with an outer diameter of 6 cm and a volume of ~ 230 mL, where the dispenser head is attached on top of it. The bottom of the dripping flask is heated to about 110°C by a constantan wire. Droplets generated by the dispenser head hit the heated bottom of the dripping flask and are immediately evaporated, which ensures that the isotopic composition of the water vapor is the same as of the source water. The dispenser head is connected to the water storage container (12 mL glass vial) via a Teflon tubing. The water is drawn to the dispenser head by capillary forces. The gas pressures in the head space of the storage container and in the dripping flask need to be the same for a reliable droplet generation by the dispenser head. Therefore, the inlet of the dripping flask is connected via a valve to the storage container by 1/16 in. PEEK tubing for pressure equilibration. The valve is only open during calibration measurements, which in combination with the small size tubing minimizes the amount of saturated air that can leave the headspace of the stor-

Water vapor isotope measurements by OA-ICOS

P. Sturm and A. Knohl

Title Page

Abstract

Introduction

Conclusions

References

Tables

Figures

◀

▶

◀

▶

Back

Close

Full Screen / Esc

Printer-friendly Version

Interactive Discussion



age container and therefore potentially alter the isotopic composition of the water. Test have shown that $\delta^2\text{H}$ and $\delta^{18}\text{O}$ values remain constant within measurement precision for a decrease of the amount of water in the storage container from 100% to 30%.

Despite the turbulence due to convection in the dripping flask, the water vapor is not well mixed at a flow rate of 500 mL min^{-1} . It was therefore necessary to add an additional buffer volume (300 mL glass flask) to reduce the variations in the signal of the water vapor mixing ratio. The calibration gas can then be directed to a purge vent which serves to setup the dripping system or to maintain the calibration gas flow during intermittent sample measurements. Alternatively, the calibration gas is directed to the analyzer for calibration measurements. All tubing in contact with moist air is 6 mm Teflon tubing, the supply line of dry air up to the dripping flask is 6 mm Synflex tubing.

The drop rate of the dripping system as well as the valves are controlled by an external computer using custom-written LabVIEW software. The raw data from the analyzer are stored on the analyzer's internal hard disk and additionally transferred via the RS-232 port to the external computer, where all calibration corrections are applied on-line (see Sect. 3) to yield $\delta^2\text{H}$ and $\delta^{18}\text{O}$ values on the VSMOW scale. The calibration measurements are performed automatically at a preset time interval. This facilitates automatic and maintenance free operation of the measurement system. A difficulty with our current calibration setup is, however, that occasionally the droplet generation stops. The reason for this is most probably the formation of vapor bubbles (cavitation) in the glass capillary of the piezo-injector due to the high acceleration of the water droplets. If this happens, the dripper needs to be set up manually again.

Water vapor isotope measurements by OA-ICOS

P. Sturm and A. Knohl

Title Page

Abstract

Introduction

Conclusions

References

Tables

Figures

◀

▶

◀

▶

Back

Close

Full Screen / Esc

Printer-friendly Version

Interactive Discussion

3 Results and discussion

3.1 Measurement precision

The stability of the system can be characterized by the Allan variance (Werle et al., 1993), which is defined as

$$\sigma_A^2(\tau) = \frac{1}{2n} \sum_{i=1}^n [y_{i+1}(\tau) - y_i(\tau)]^2 \quad (2)$$

where τ is the averaging time, y_i is the average value of the measurements in the averaging interval i and n is the total number of averaging intervals for a given τ . Figure 2 shows the Allan deviation (square root of the Allan variance) for $\delta^2\text{H}$ and $\delta^{18}\text{O}$ as a function of the averaging time. Calibration air with a H_2O mixing ratio of 14 000 ppm was used for this test. The precision at one second is about 0.6‰ for $\delta^2\text{H}$ and 0.25‰ for $\delta^{18}\text{O}$. At 15 s averaging time, which is an appropriate averaging time for chamber or profile measurements, the respective Allan deviation is 0.16‰ and 0.08‰ for $\delta^2\text{H}$ and $\delta^{18}\text{O}$. The optimum averaging time derived from the Allan plots is 10–15 min. The 15 min Allan deviation is 0.04‰ for $\delta^2\text{H}$ and 0.03‰ for $\delta^{18}\text{O}$. For longer averaging times the variance increases again due to drifts in the signal, probably caused by temperature variations.

The precision is also dependent on the water vapor mixing ratio (Fig. 3). The one second standard deviation is smallest at high mixing ratios and increases proportional to the inverse of the mixing ratio leading to a strong increase below 5000 ppm.

The best analytical precision of liquid water measurements that can be obtained by isotope ratio mass spectrometric techniques is about 0.5–1.0‰ for $\delta^2\text{H}$ and 0.05–0.10‰ for $\delta^{18}\text{O}$ (Epstein and Mayeda, 1953; Coplen et al., 1991; Angert et al., 2008; Uemura et al., 2008). The 15 s precision of the WVIA is therefore comparable (for $\delta^{18}\text{O}$) or better (for $\delta^2\text{H}$) compared to conventional IRMS measurements, which highlights the potential for fast and precise water vapor isotope measurements.

Title Page

Abstract

Introduction

Conclusions

References

Tables

Figures

◀

▶

◀

▶

Back

Close

Full Screen / Esc

Printer-friendly Version

Interactive Discussion



3.2 Response time

Figure 4 shows the response time of a step change when inlet air is switched from sample to calibration at a flow rate of 800 mL min^{-1} . The time lag after the switch, which is given by the length of the inlet tubing and the volume of the inlet filters, is $\sim 4 \text{ s}$.

5 The time constant of the exponential change is $\sim 3 \text{ s}$ for the isotope ratios as well as for the water vapor mixing ratio. This is in good agreement with the cell exchange time estimated from the flow rate and the cell volume and indicates that there is no discernible memory effect associated with adsorption/desorption processes of the Teflon tubing or inside the instrument.

10 Additional tests with Synflex tubing showed, however, that Synflex tubing is unsuitable for water isotope measurements. Synflex is a composite polyethylene/aluminum tubing with an ethylene copolymer coating on its inside and it is widely used for atmospheric air sampling applications.

15 Instead of the usual 1.5 m of Teflon tubing which connects the calibration unit and the WVIA we have used various lengths of Synflex and Teflon tubing (6 mm outer diameter). Figure 5 shows the response time for a switch from sample to calibration air with $\sim 27 \text{ m}$ of Synflex tubing and $\sim 32 \text{ m}$ of Teflon tubing, respectively, at a flow rate of 450 mL min^{-1} . Synflex has considerably longer retention times for H_2O and $\delta^{18}\text{O}$ compared to Teflon (middle and bottom panel in Fig. 5). Most notably there is a large fractionation in $\delta^2\text{H}$ with Synflex tubing (top panel in Fig. 5), which persists for very long time periods. Even after 30 min the $\delta^2\text{H}$ did not reach the target value. Heating the Synflex tubing to $\sim 40^\circ\text{C}$ did not reduce this fractionation. Thus, Synflex tubing is not recommended as a sample intake line for water vapor isotope analyses.

3.3 Concentration dependence

25 An important characteristic of any isotope ratio spectrometer is the instrument response to changing concentration at constant isotopic composition. In order to evaluate the concentration dependence of the isotope ratios we have analyzed standard water

Title Page

Abstract

Introduction

Conclusions

References

Tables

Figures

◀

▶

◀

▶

Back

Close

Full Screen / Esc

Printer-friendly Version

Interactive Discussion



at different H₂O mixing ratios with our calibration system (Fig. 6). The drop rate of the dripping system and thereby the mixing ratio was changed from low to high and back to low values (“step pyramid”) to ensure that there is no hysteresis behavior. As shown in Fig. 6 (black dots) there is a pronounced nonlinearity of several per mille in the δ -values for both isotope ratios in a concentration range of 2000–27 000 ppm. The shape of this nonlinearity is different for $\delta^2\text{H}$ and $\delta^{18}\text{O}$.

To demonstrate that this concentration dependence stems from the laser spectrometer and not from our calibration system we compared the results from the dripping system with data obtained with a dew point generator (grey dots in Fig. 6). If the temperature dependent equilibrium fractionation at the liquid/gaseous phase change (Majoube, 1971) as well as the Rayleigh-type enrichment of the remaining water in the reservoir of the dew point generator is taken into account, the resulting H₂O dependences are very similar to the results from the dripping system, indicating that the nonlinearity is not due to the water vapor generation with our dripper. The concentration dependence is rather related to the spectral fitting procedure. Theoretical uncertainties and approximations in the spectroscopic parameters and the fitting model which are used to calculate the isotopologue mixing ratios as well as interferences from adjacent adsorption lines are likely causes of H₂O dependences. Brand et al. (2009) reported similar nonlinearities (comparable in magnitude, but different in shape) from another laser spectrometer based on cavity ring-down spectroscopy.

As an additional test the water vapor generated with the dripping system and analyzed by the WVIA has been trapped at the outlet of the analyzer. Two cold traps immersed in liquid nitrogen and placed in series upstream of the pump were used to freeze out the water. The second cold trap was used to check the efficiency of the trapping and we found that all water was retained in the first cold trap. The trapped water along with the source water was then analyzed by IRMS. The aims of this experiment were to test the assumption that no fractionation is occurring within the calibration/analysis system, i.e. that the isotopic signature of the source water is the same as of the trapped water. The dashed lines in Fig. 6 show the isotopic composition of

Water vapor isotope measurements by OA-ICOS

P. Sturm and A. Knohl

Title Page

Abstract

Introduction

Conclusions

References

Tables

Figures

◀

▶

◀

▶

Back

Close

Full Screen / Esc

Printer-friendly Version

Interactive Discussion



**Water vapor isotope
measurements by
OA-ICOS**

P. Sturm and A. Knohl

Title Page

Abstract

Introduction

Conclusions

References

Tables

Figures

◀

▶

◀

▶

Back

Close

Full Screen / Esc

Printer-friendly Version

Interactive Discussion



the source water and the open squares are the results from three trapping experiments at $\sim 20\,000$ ppm and $\sim 10\,000$ ppm. The water vapor was frozen out during 3 to 6 h in order to obtain a sufficient amount of water for subsequent analysis by IRMS. Possible fractionation effects when unfreezing the cold trap and decanting small amounts of water into vials lead to additional scatter in the IRMS results. Nevertheless, there is no systematic difference between the source water and the trapped water, which confirms that the generated water vapor measured in the analyzer has the same isotopic signature as the source water. The WVIA data were obtained with the uncalibrated instrument resulting in an offset compared to the calibrated IRMS results.

The nonlinearity curves preserved the same shape for different standard waters ranging from -190‰ to -80‰ in $\delta^2\text{H}$ and from -25‰ to -5‰ in $\delta^{18}\text{O}$ (not shown). It is therefore sufficient to characterize the instrumental response to changing water concentrations with one water standard. Tests at ambient temperatures between 11°C and 33°C (see Sect. 3.4) revealed that the nonlinearity correction is not dependent on the temperature either. Therefore, in the short term the nonlinearity is a robust feature and highly reproducible. Unfortunately, it does however vary with mirror contamination. Despite $0.5\ \mu\text{m}$ inlet filters the mirror reflectivity can change over time and with continued use of the instrument. We observed, for example, a decline in the ring-down time (at a fixed H_2O mixing ratio) of about $1\ \mu\text{s}$ probably due to the use of a contaminated pressurized air tank. This significantly changed the nonlinearity curve for $\delta^2\text{H}$, but not for $\delta^{18}\text{O}$. The ring-down time then gradually increased again within about two weeks after replacement of this air tank. It is therefore necessary to regularly determine the concentration dependence and to take note of changes in the ring-down time.

The corrections derived from the nonlinearity calibration and an arbitrary reference water mixing ratio of $15\,000$ ppm are applied on-line to the raw data and they amount up to 5‰ for $\delta^2\text{H}$ and up to 2‰ for $\delta^{18}\text{O}$. We estimated the uncertainty in $\delta^{18}\text{O}$ and $\delta^2\text{H}$ stemming from this correction from 15 subsequent nonlinearity measurements over 3.5 h, where we assumed the nonlinearity curves to be constant. The standard deviation of the nonlinearity correction estimated from 15 measurements over the range

Water vapor isotope measurements by OA-ICOS

P. Sturm and A. Knohl

of 4500 to 16 000 ppm amounts up to 0.47‰ for $\delta^2\text{H}$ and 0.27‰ for $\delta^{18}\text{O}$ depending on the water mixing ratio (Table 1). Depending on the expected water concentrations it is advantageous to calibrate the instrument over the expected concentration range. This allows to fit a low order polynomial function and might decrease the uncertainty associated with the correcting factors.

It is important to note that it is essential to quantify the concentration dependence when using such a water vapor isotope analyzer. As an example, if we calculate the deuterium excess ($d = \delta^2\text{H} - 8 \times \delta^{18}\text{O}$) from uncorrected $\delta^2\text{H}$ and $\delta^{18}\text{O}$ for water with the same isotopic signature but measured at different H_2O mixing ratios we could be misled by up to 25%.

3.4 Temperature sensitivity

Typical diurnal variations of the ambient temperature in our lab of $\pm 1.5^\circ\text{C}$ are attenuated by the temperature control of the cavity to about $\pm 0.25^\circ\text{C}$. In order to evaluate the influence of the room temperature on the isotope ratio measurements, we performed tests in plant growth chambers, where the ambient temperature can be controlled. While standard water from the dripper was continuously measured by the WVIA, which was placed inside the growth chamber, the room temperature in the chamber was set to follow a diurnal cycle between 19°C and 29°C . The calibration system was either placed also inside or outside of the growth chamber to distinguish between potential temperature sensitivities of the WVIA and the calibration system. Since we could not observe a difference in the overall temperature sensitivity with the calibration system either placed inside or outside the growth chamber, we conclude that the isotope ratios of the water vapor generated by the dripper are temperature insensitive. However, there is a temperature sensitivity of the measured $\delta^2\text{H}$ and $\delta^{18}\text{O}$ of $(-0.37 \pm 0.03)\text{‰}/^\circ\text{C}$ and $(-0.24 \pm 0.03)\text{‰}/^\circ\text{C}$, respectively, in a temperature range of $19\text{--}29^\circ\text{C}$ (Fig. 7).

We have observed that for ambient temperatures below $\sim 22^\circ\text{C}$ the cavity temperature does not reach the setpoint any more, presumably because of insufficient heating

[Title Page](#)[Abstract](#)[Introduction](#)[Conclusions](#)[References](#)[Tables](#)[Figures](#)[◀](#)[▶](#)[◀](#)[▶](#)[Back](#)[Close](#)[Full Screen / Esc](#)[Printer-friendly Version](#)[Interactive Discussion](#)

power at colder room temperatures². The cavity temperature then closely follows room temperature variations. Interestingly, the isotope ratios are linearly correlated over the whole temperature range with the room temperature, but not with the cavity temperature. This indicates that the gas temperature in the cavity (i.e. the temperature dependent line strength of the absorption lines) is not the main driver of the temperature sensitivity. Temperature changes of the optics, the laser or other electronic components are likely causing the temperature sensitivity.

Currently, we do not routinely measure the ambient temperature, but because the temperature of the room where the instrument is placed in is always above 22°C, we use the temperature measured in the cavity which is recorded continuously to correct for the temperature sensitivity. For cavity temperatures between 46.5–47.5°C we derived correction factors of $(-2.03 \pm 0.19)\%$ per °C change in cavity temperature for $\delta^2\text{H}$ and $(-1.30 \pm 0.19)\%$ for $\delta^{18}\text{O}$. The temperature correction is calculated relative to an arbitrary reference temperature of 47.0°C and applied on-line to the raw data.

3.5 H₂O mixing ratio calibration

The water vapor mixing ratio of the calibration gas can be estimated from the mass flow rate of the gas, the dripping rate and the nominal droplet size of the dripping device. Uncertainties in all these variables, however, will restrict the accuracy of such an estimation. A more precise determination of the water vapor mixing ratio can be obtained from a moist air stream with a known dew point.

We are using a dew point generator (LI-610, LI-COR) to independently determine water vapor mixing ratios. Air is pumped through the dew point generator by the internal pump and then directed to the WVIA. A small portion of the air stream is vented to the lab to prevent over-pressure. Flow resistance due to plumbing still causes a small over-pressure at the place where the air is bubbled through the water. This over-pressure is

²The temperature control of the measurement cell has recently been improved in an updated version of the WVIA (D. Baer, personal communication, 2009).

Water vapor isotope measurements by OA-ICOS

P. Sturm and A. Knohl

Title Page

Abstract

Introduction

Conclusions

References

Tables

Figures

◀

▶

◀

▶

Back

Close

Full Screen / Esc

Printer-friendly Version

Interactive Discussion



estimated to be smaller than 1 hPa. The water vapor mixing ratio can then be calculated from the the air pressure and the temperature dependent saturation vapor pressure of water vapor in air (Buck, 1981).

Figure 8 shows the dew point temperature and the corresponding water vapor mixing ratio determined by the dew point generator versus the mixing ratio measured by the WVIA using the factory pre-calibration. The WVIA shows an excellent linearity over the range of 7000–29 000 ppm. The offset of the linear slope as well as the residuals from the fit are smaller than the stated accuracy of the dew point generator, which is 100–325 ppm over this range. Such water vapor mixing ratio calibrations have only been performed occasionally. No drifts have been observed so far, allowing for very accurate water mixing ratio measurements.

3.6 $\delta^2\text{H}$ and $\delta^{18}\text{O}$ calibration

In order to link the δ -values to an absolute scale, calibration with water of known isotopic composition is required. We have used five different local water standards to calibrate the $\delta^2\text{H}$ and $\delta^{18}\text{O}$ results of the WVIA. These water standard span a range of -190 to -80% for $\delta^2\text{H}$ and -5 to -25% for $\delta^{18}\text{O}$. The waters have been analyzed in our laboratory by IRMS (Gehre et al., 2004) to get independent δ -values on the international VSMOW scale. IRMS measurements were made using a high-temperature conversion/elemental analyser coupled on-line via a ConFlo III interface to a Delta^{PLUS} XP mass spectrometer (Thermo Fisher Scientific Inc., Germany). Figure 9 presents the resulting calibration curves for the two isotopic species. The δ -values of the WVIA are reported using the factory pre-calibration. A weighted least squares fit through the data gives $\delta^2\text{H}_{\text{IRMS}}=(1.013\pm 0.011)\delta^2\text{H}_{\text{WVIA}}-(5.82\pm 1.53)$ and $\delta^{18}\text{O}_{\text{IRMS}}=(1.007\pm 0.019)\delta^{18}\text{O}_{\text{WVIA}}-(2.92\pm 0.32)$. The high correlation ($R^2>0.99$) demonstrates the linear response of the δ -values on the VSMOW scale within the range of our water standards.

The uncertainty of these calibration equations results from both IRMS and WVIA

Water vapor isotope measurements by OA-ICOS

P. Sturm and A. Knohl

Title Page

Abstract

Introduction

Conclusions

References

Tables

Figures

◀

▶

◀

▶

Back

Close

Full Screen / Esc

Printer-friendly Version

Interactive Discussion



uncertainties. From that we estimate an uncertainty of the calibrated δ -value on the VSMOW scale of 0.44–0.73‰ for $\delta^2\text{H}$ and 0.14–0.20‰ for $\delta^{18}\text{O}$ within the calibrated range (Table 1). Continual measurements of calibrated water standards will likely reduce this uncertainty.

5 3.7 Long-term precision

As a measure of the long-term precision of the WVIA we repeatedly analyzed a water standard during an ongoing measurement campaign. Along with a carbon dioxide isotope analyzer the WVIA was deployed for an ecophysiological experiment in our laboratory and continuously measured the isotope composition of gas exchange water fluxes of small beech trees. The first six minutes of every hour were allocated to calibration measurements of the carbon dioxide isotope analyzer and we have used this time period to perform water standard measurements. Calibration air with a water vapor mixing ratio of about 11 000 ppm was fed to the analyzer and the data of the last two minutes of each six minute period were averaged to calculate $\delta^2\text{H}$ and $\delta^{18}\text{O}$. Figure 10 shows the time series of these calibration measurements. A linearity calibration was performed every day at midnight and an according linearity correction was applied as described in Sect. 3.3. Due to the high short-term precision of these measurements a small diurnal cycle with an amplitude of about 0.4‰ becomes apparent in the $\delta^2\text{H}$ record. It is not clear yet what is causing this behavior. The room temperature during this period varied between 26 and 27°C and the resulting small temperature correction was also applied to the data. We speculate that either other not yet accounted for temperature effects or the influence of the intermittent sample measurements is responsible for this diurnal cycle. The intermittent sample H_2O mixing ratio also followed diurnal variations and might have conditioned the measurement cell at different water concentrations leading to some kind of memory effect. The $\delta^{18}\text{O}$ data show periods with similar scatter as the $\delta^2\text{H}$, but then also very stable periods (21–24 June, $\sigma=0.09\text{‰}$) and an abrupt shift after a gap of several hour where the dripper had stopped working (24 June). Remarkably, this shift to more negative values does not

Water vapor isotope measurements by OA-ICOS

P. Sturm and A. Knohl

Title Page

Abstract

Introduction

Conclusions

References

Tables

Figures

◀

▶

◀

▶

Back

Close

Full Screen / Esc

Printer-friendly Version

Interactive Discussion



appear in the $\delta^2\text{H}$ data.

Notwithstanding the yet unidentified sources of these variations, the standard deviation of all 199 measurements during the 12 days is 0.38‰ for $\delta^2\text{H}$ and 0.25‰ for $\delta^{18}\text{O}$, respectively. These values represent the long-term precision that can currently be achieved with our measurement set-up.

4 Conclusions

The different sources of uncertainty contributing to the overall performance of the WVIA and its calibration system are summarized in Table 1. The short-term (15 s average) precision of 0.16‰ for $\delta^2\text{H}$ and 0.08‰ for $\delta^{18}\text{O}$ is comparable or better than what can be achieved using classical IRMS techniques. However, the short-term precision is not necessarily the limiting factor of the instrument's performance and can therefore not be used as the only measure to characterize the potential of the analyzer. Primarily, the concentration dependence of the isotope ratios is a crucial aspect. If this is not taken into account, then the error arising from the non-linear behavior of the WVIA can amount to several per mil and potentially exceed the signal that one would like to measure. With an appropriate calibration system the linearity of the instrument can be determined and a respective correction can be applied. Still, such a correction adds to the total measurement error.

Another uncertainty stems from temperature sensitivity of the instrument. Temperature corrections are dependent on the magnitude of the temperature variations that the instrument is exposed to. Hence, minimizing ambient temperature fluctuations helps to reduce the contribution of the temperature sensitivity to the total measurement error.

The resulting long-term precision estimated from repeated water standard measurements is 0.38‰ for $\delta^2\text{H}$ and 0.25‰ for $\delta^{18}\text{O}$. In addition, the accuracy of the water vapor isotope measurements was evaluated with different standard waters that have been analyzed by isotope ratio mass spectrometry showing a linear response of the δ -values on the VSMOW scale.

Water vapor isotope measurements by OA-ICOS

P. Sturm and A. Knohl

Title Page

Abstract

Introduction

Conclusions

References

Tables

Figures

◀

▶

◀

▶

Back

Close

Full Screen / Esc

Printer-friendly Version

Interactive Discussion



In summary, we have shown that off-axis integrated cavity output spectroscopy combined with a reliable calibration system provides accurate high resolution water vapor isotope measurements. Such continuous in-situ measurements of $\delta^2\text{H}$ and $\delta^{18}\text{O}$ in water vapor may open new prospects for ecological and hydrological field studies. For example, they offer a tool for online gas exchange measurements of water vapor isotopes.

Acknowledgements. This project was funded by the EC Marie Curie Excellence grant ISOCYCLE under contract No. MEXT-CT-2006-042268. We thank R. A. Werner (Grassland Isolab, ETH Zürich) for IRMS analyses, P. Plüss (Grassland Group, ETH Zürich) for assistance with electronic components and D. Baer (Los Gatos Research Inc.) for technical support.

References

- Andersen, K., Azuma, N., Barnola, J., Bigler, M., Biscaye, P., Caillon, N., Chappellaz, J., Clausen, H., Dahl-Jensen, D., Fischer, H., et al.: High-resolution record of Northern Hemisphere climate extending into the last interglacial period, *Nature*, 431, 147–151, 2004. 2056
- Angert, A., Lee, J., and Yakir, D.: Seasonal variations in the isotopic composition of near-surface water vapour in the eastern Mediterranean, *Tellus B*, 60, 674–684, doi:10.1111/j.1600-0889.2008.00357.x, 2008. 2063
- Baer, D., Paul, J., Gupta, M., and O’Keefe, A.: Sensitive absorption measurements in the near-infrared region using off-axis integrated-cavity-output spectroscopy, *Appl. Phys. B-Lasers O.*, 75, 261–265, doi:10.1007/s00340-002-0971-z, 2002. 2057, 2058
- Barbour, M.: Stable oxygen isotope composition of plant tissue: a review, *Funct. Plant Biol.*, 34, 83–94, doi:10.1071/FP06228, 2007. 2056
- Brand, W. A., Geilmann, H., Crosson, E. R., and Rella, C. W.: Cavity ring-down spectroscopy versus high-temperature conversion isotope ratio mass spectrometry and a case study on $\delta^2\text{H}$ and $\delta^{18}\text{O}$ of pure water samples and alcohol/water mixtures, *Rapid Commun. Mass Sp.*, 23, 1879–1884, doi:10.1002/rcm.4083, 2009. 2060, 2065
- Buck, A.: New equations for computing vapor pressure and enhancement factor, *J. Appl. Meteorol.*, 20, 1527–1532, 1981. 2069

Water vapor isotope measurements by OA-ICOS

P. Sturm and A. Knohl

Title Page

Abstract

Introduction

Conclusions

References

Tables

Figures

◀

▶

◀

▶

Back

Close

Full Screen / Esc

Printer-friendly Version

Interactive Discussion



- Coplen, T., Wildman, J., and Chen, J.: Improvements in the gaseous hydrogen-water equilibration technique for hydrogen isotope-ratio analysis, *Anal. Chem.*, 63, 910–912, 1991. 2063
- Epstein, S. and Mayeda, T.: Variation of O^{18} content of waters from natural sources, *Geochim. Cosmochim. Ac.*, 4, 213–224, doi:10.1016/0016-7037(53)90051-9, 1953. 2063
- 5 Farquhar, G., Cernusak, L., and Barnes, B.: Heavy Water Fractionation during Transpiration, *Plant Physiol.*, 143, 11–18, doi:10.1104/pp.106.093278, 2007. 2056
- Gat, J.: Oxygen and hydrogen isotopes in the hydrologic cycle, *Annu. Rev. Earth Pl. Sc.*, 24, 225–262, 1996. 2056
- Gehre, M., Geilmann, H., Richter, J., Werner, R., and Brand, W.: Continuous flow $^2H/^1H$ and $^{18}O/^{16}O$ analysis of water samples with dual inlet precision, *Rapid Commun. Mass Sp.*, 18, 2650–2660, doi:10.1002/rcm.1672, 2004. 2069
- 10 Gianfrani, L., Gagliardi, G., van Burgel, M., and Kerstel, E.: Isotope analysis of water by means of near infrared dual-wavelength diode laser spectroscopy, *Opt. Express*, 11, 1566–1576, 2003. 2057
- 15 Gonfiantini, R.: Standards for stable isotope measurements in natural compounds, *Nature*, 271, 534–536, 1978. 2059
- Gupta, P., Noone, D., Galewsky, J., Sweeney, C., and Vaughn, B. H.: Demonstration of high-precision continuous measurements of water vapor isotopologues in laboratory and remote field deployments using wavelength-scanned cavity ring-down spectroscopy (WS-CRDS) technology, *Rapid Commun. Mass Sp.*, 23, 2534–2542, doi:10.1002/rcm.4100, 2009. 2057
- 20 Han, L., Groning, M., Aggarwal, P., and Helliker, B.: Reliable determination of oxygen and hydrogen isotope ratios in atmospheric water vapour adsorbed on 3A molecular sieve, *Rapid Commun. Mass Sp.*, 20, 3612–3618, doi:10.1002/rcm.2772, 2006. 2057
- Iannone, R. Q., Romanini, D., Kassi, S., Meijer, H. A., and Kerstel, E. R. T.: A microdrop generator for the calibration of a water vapor isotope ratio spectrometer, *J. Atmos. Ocean. Tech.*, 26, 1275–1288, doi:10.1175/2008JTECHA1218.1, 2009. 2058, 2061
- 25 Kerstel, E., van Trigt, R., Dam, N., Reuss, J., and Meijer, H.: Simultaneous determination of the $^2H/^1H$, $^{17}O/^{16}O$, and $^{18}O/^{16}O$ isotope abundance ratios in water by means of laser spectrometry, *Anal. Chem.*, 71, 5297–5303, 1999. 2057
- 30 Kerstel, E., Gagliardi, G., Gianfrani, L., Meijer, H., van Trigt, R., and Ramaker, R.: Determination of the $^2H/^1H$, $^{17}O/^{16}O$, and $^{18}O/^{16}O$ isotope ratios in water by means of tunable diode laser spectroscopy at $1.39\ \mu m$, *Spectrochim. Acta A*, 58, 2389–2396, 2002. 2057
- Kerstel, E., Iannone, R., Chenevier, M., Kassi, S., Jost, H., and Romanini, D.: A water isotope

Water vapor isotope measurements by OA-ICOSP. Sturm and A. Knohl

[Title Page](#)[Abstract](#)[Introduction](#)[Conclusions](#)[References](#)[Tables](#)[Figures](#)[◀](#)[▶](#)[◀](#)[▶](#)[Back](#)[Close](#)[Full Screen / Esc](#)[Printer-friendly Version](#)[Interactive Discussion](#)

Water vapor isotope measurements by OA-ICOS

P. Sturm and A. Knohl

Title Page

Abstract

Introduction

Conclusions

References

Tables

Figures

◀

▶

◀

▶

Back

Close

Full Screen / Esc

Printer-friendly Version

Interactive Discussion

(^2H , ^{17}O , and ^{18}O) spectrometer based on optical feedback cavity-enhanced absorption for in situ airborne applications, *Appl. Phys. B-Lasers O.*, 85, 397–406, doi:10.1007/s00340-006-2356-1, 2006. 2060

Lee, X., Sargent, S., Smith, R., and Tanner, B.: In Situ Measurement of the Water Vapor $^{18}\text{O}/^{16}\text{O}$ Isotope Ratio for Atmospheric and Ecological Applications, *J. Atmos. Ocean. Tech.*, 22, 555–565, 2005. 2057, 2060

Lis, G., Wassenaar, L. I., and Hendry, M. J.: High-Precision Laser Spectroscopy D/H and $^{18}\text{O}/^{16}\text{O}$ Measurements of Microliter Natural Water Samples, *Anal. Chem.*, 80, 287–293, doi:10.1021/ac701716q, 2008. 2057, 2060

Majoube, M.: Fractionnement en oxygène-18 et en deutérium entre l'eau et sa vapeur, *J. Chim. Phys.*, 68, 1423–1436, 1971. 2065

Rothman, L., Jacquemart, D., Barbe, A., Chris Benner, D., Birk, M., Brown, L., Carleer, M., Chackerian, C., Chance, K., Coudert, L., et al.: The HITRAN 2004 molecular spectroscopic database, *J. Quant. Spectrosc. Ra.*, 96, 139–204, doi:10.1016/j.jqsrt.2004.10.008, 2005. 2058

Uemura, R., Matsui, Y., Yoshimura, K., Motoyama, H., and Yoshida, N.: Evidence of deuterium excess in water vapor as an indicator of ocean surface conditions, *J. Geophys. Res.*, 113, D19114, doi:10.1029/2008JD010209, 2008. 2063

Wang, L., Caylor, K., and Dragoni, D.: On the calibration of continuous, high-precision $\delta^{18}\text{O}$ and $\delta^2\text{H}$ measurements using an off-axis integrated cavity output spectrometer, *Rapid Commun. Mass Sp.*, 23, 530–536, doi:10.1002/rcm.3905, 2009. 2060

Wen, X., Sun, X., Zhang, S., Yu, G., Sargent, S., and Lee, X.: Continuous measurement of water vapor D/H and $^{18}\text{O}/^{16}\text{O}$ isotope ratios in the atmosphere, *J. Hydrol.*, 349, 489–500, doi:10.1016/j.jhydrol.2007.11.021, 2008. 2060

Werle, P., Mücke, R., and Slemr, F.: The limits of signal averaging in atmospheric trace-gas monitoring by tunable diode-laser absorption spectroscopy (TDLAS), *Appl. Phys. B-Lasers O.*, 57, 131–139, 1993. 2063

Water vapor isotope measurements by OA-ICOS

P. Sturm and A. Knohl

Table 1. Different sources of uncertainty contributing to the overall performance.

Source of uncertainty	Estimated uncertainty (‰)	
	$\delta^2\text{H}$	$\delta^{18}\text{O}$
Short-term precision ^a	0.16	0.08
Concentration dependence ^b	0–0.47	0–0.27
Temperature sensitivity ^b	0–0.10	0–0.09
Long-term precision	0.38	0.25
VSMOW calibration ^b	0.44–0.73	0.14–0.20

^a Allan deviation at 15 s averaging time.

^b Estimated from the uncertainty of the fitted correction/calibration function over the calibrated range.

Title Page

Abstract

Introduction

Conclusions

References

Tables

Figures

◀

▶

◀

▶

Back

Close

Full Screen / Esc

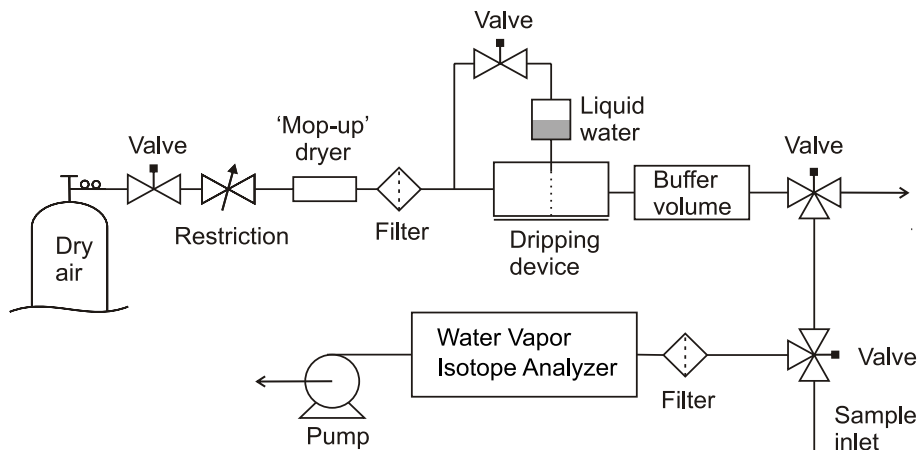
Printer-friendly Version

Interactive Discussion



Water vapor isotope measurements by OA-ICOS

P. Sturm and A. Knohl

**Fig. 1.** Schematic diagram of the gas handling setup.[Title Page](#)[Abstract](#)[Introduction](#)[Conclusions](#)[References](#)[Tables](#)[Figures](#)[◀](#)[▶](#)[◀](#)[▶](#)[Back](#)[Close](#)[Full Screen / Esc](#)[Printer-friendly Version](#)[Interactive Discussion](#)

Water vapor isotope measurements by OA-ICOS

P. Sturm and A. Knohl

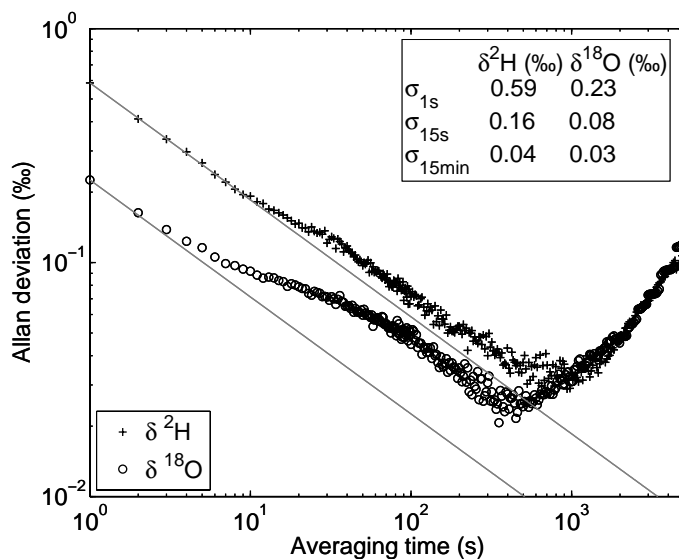


Fig. 2. Allan plots of $\delta^2\text{H}$ (plus signs) and $\delta^{18}\text{O}$ (circles) as a measurement of signal stability. The black lines show the theoretical slope for white noise. The upper insert shows Allan deviations (square root of the Allan variance) for different averaging times.

[Title Page](#)[Abstract](#)[Introduction](#)[Conclusions](#)[References](#)[Tables](#)[Figures](#)[◀](#)[▶](#)[◀](#)[▶](#)[Back](#)[Close](#)[Full Screen / Esc](#)[Printer-friendly Version](#)[Interactive Discussion](#)

Water vapor isotope measurements by OA-ICOS

P. Sturm and A. Knohl

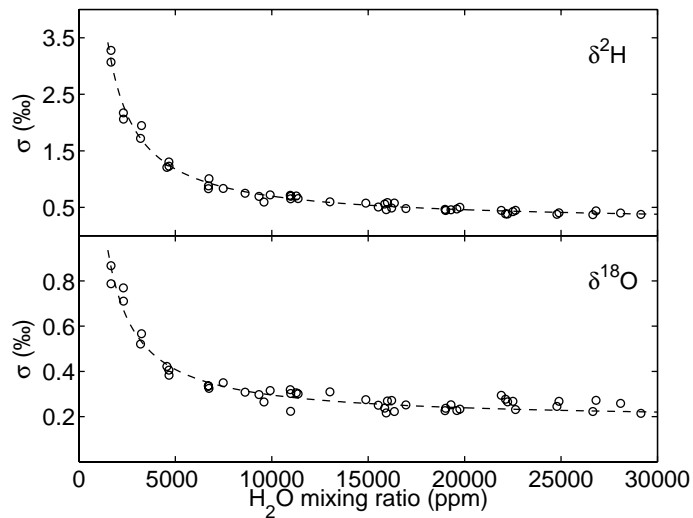


Fig. 3. Standard deviations of 1 s measurements of $\delta^{2}\text{H}$ (top) and $\delta^{18}\text{O}$ (bottom) as a function of H_2O mixing ratio. The dotted lines show $1/x$ -fits.

[Title Page](#)[Abstract](#)[Introduction](#)[Conclusions](#)[References](#)[Tables](#)[Figures](#)[◀](#)[▶](#)[◀](#)[▶](#)[Back](#)[Close](#)[Full Screen / Esc](#)[Printer-friendly Version](#)[Interactive Discussion](#)

Water vapor isotope measurements by OA-ICOS

P. Sturm and A. Knohl

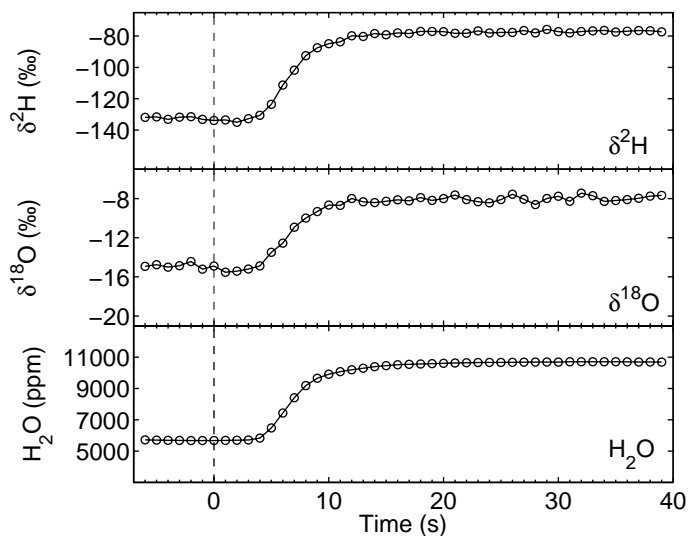


Fig. 4. Response time of a step change (at $t=0$ s) when inlet air is switched from sample to calibration at a flow rate of 800 mL min^{-1} for $\delta^2\text{H}$ (top), $\delta^{18}\text{O}$ (middle) and H_2O (bottom). The time lag after the switch is ~ 4 s and the time constant of the exponential change is ~ 3 s.

[Title Page](#)[Abstract](#)[Introduction](#)[Conclusions](#)[References](#)[Tables](#)[Figures](#)[◀](#)[▶](#)[◀](#)[▶](#)[Back](#)[Close](#)[Full Screen / Esc](#)[Printer-friendly Version](#)[Interactive Discussion](#)

Water vapor isotope measurements by OA-ICOS

P. Sturm and A. Knohl

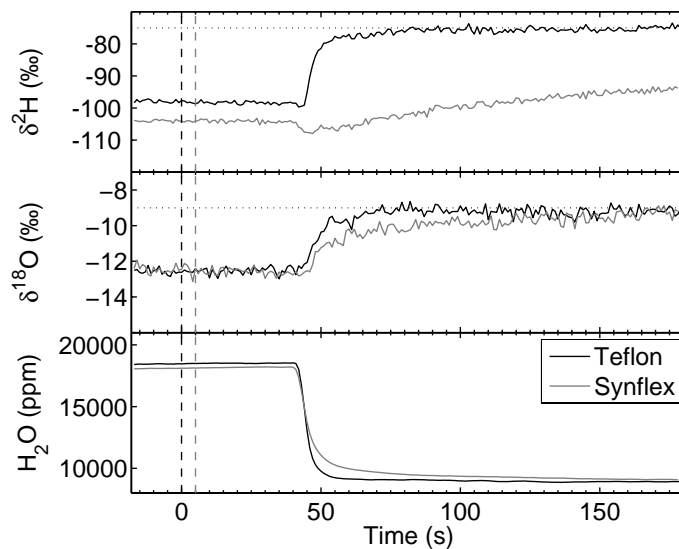


Fig. 5. Response time of a step change when inlet air is switched from sample to calibration and led to the WVIA through ~ 32 m of Teflon tubing (black line) or ~ 27 m of Synflex tubing (grey line), respectively, at a flow rate of 450 mL min^{-1} . The Synflex data are shifted by 5 s to account for the smaller time lag after the switch (dashed lines) due to the shorter tubing length. The dotted lines are the target values of the isotope ratios.

[Title Page](#)[Abstract](#)[Introduction](#)[Conclusions](#)[References](#)[Tables](#)[Figures](#)[◀](#)[▶](#)[◀](#)[▶](#)[Back](#)[Close](#)[Full Screen / Esc](#)[Printer-friendly Version](#)[Interactive Discussion](#)

Water vapor isotope measurements by OA-ICOS

P. Sturm and A. Knohl

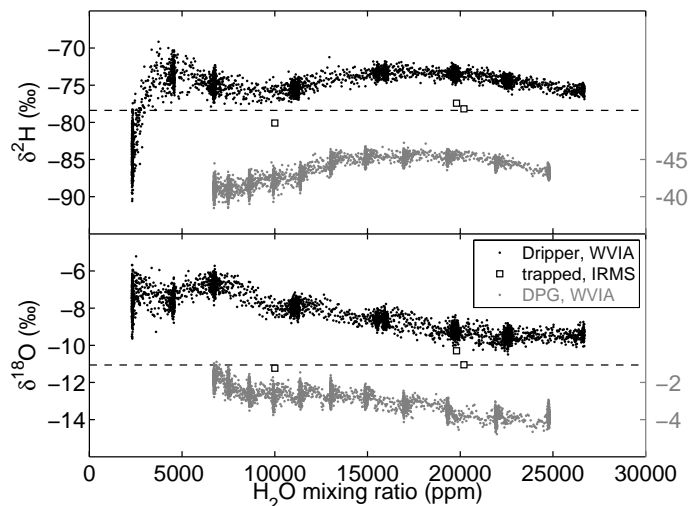


Fig. 6. Nonlinearity of $\delta^2\text{H}$ (black dots, top) and $\delta^{18}\text{O}$ (black dots, bottom) with changing H_2O mixing ratio. For comparison results from water vapor generated by a dew point generator (DPG) are shown (grey dots, corrected for equilibrium and Rayleigh fractionation). The different range in δ -values for the dew point generator compared to the dripper is due to different source water that was used for this test. Water trapped at the outlet of the WVIA and measured by IRMS (squares) is compared to the isotopic signature of the source water (dashed lines). Error bars of the IRMS measurements are smaller than the used symbols.

[Title Page](#)[Abstract](#)[Introduction](#)[Conclusions](#)[References](#)[Tables](#)[Figures](#)[◀](#)[▶](#)[◀](#)[▶](#)[Back](#)[Close](#)[Full Screen / Esc](#)[Printer-friendly Version](#)[Interactive Discussion](#)

Water vapor isotope measurements by OA-ICOS

P. Sturm and A. Knohl

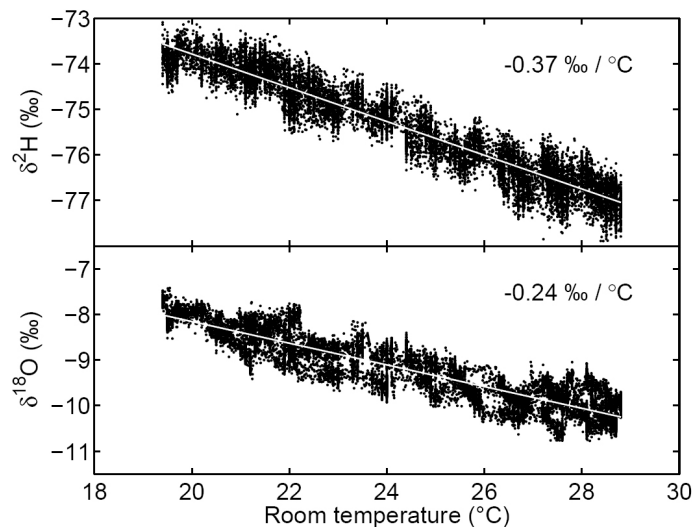


Fig. 7. Sensitivity to room temperature variations for $\delta^2\text{H}$ (top) and $\delta^{18}\text{O}$ (bottom). The dots are 10 s averaged data and the ordinary least squares fits yield slopes of $-0.37\text{‰}/^\circ\text{C}$ ($R^2=0.92$) and $-0.24\text{‰}/^\circ\text{C}$ ($R^2=0.82$) for $\delta^2\text{H}$ and $\delta^{18}\text{O}$, respectively (white lines).

Title Page

Abstract

Introduction

Conclusions

References

Tables

Figures

◀

▶

◀

▶

Back

Close

Full Screen / Esc

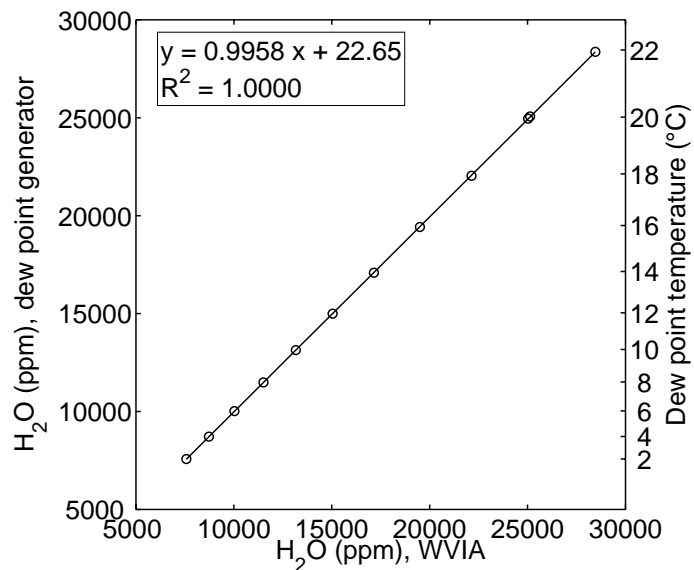
Printer-friendly Version

Interactive Discussion



Water vapor isotope measurements by OA-ICOS

P. Sturm and A. Knohl

**Fig. 8.** Calibration of the water vapor mixing ratio with a dew point generator.[Title Page](#)[Abstract](#)[Introduction](#)[Conclusions](#)[References](#)[Tables](#)[Figures](#)[◀](#)[▶](#)[◀](#)[▶](#)[Back](#)[Close](#)[Full Screen / Esc](#)[Printer-friendly Version](#)[Interactive Discussion](#)

Water vapor isotope measurements by OA-ICOS

P. Sturm and A. Knohl

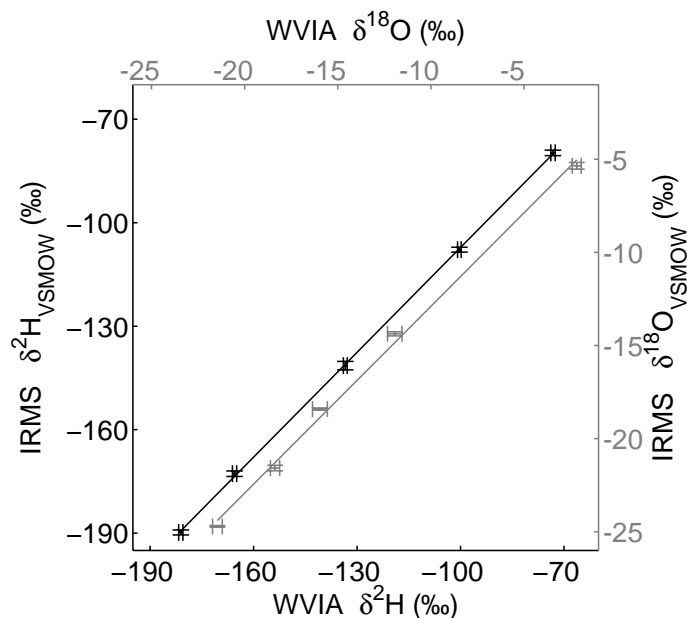


Fig. 9. Calibration of $\delta^2\text{H}$ (black) and $\delta^{18}\text{O}$ (grey) with different water standards. Weighted least squares fit through the data results in $\delta^2\text{H}_{\text{IRMS}} = (1.013 \pm 0.011) \delta^2\text{H}_{\text{WVIA}} - (5.82 \pm 1.53)$ and $\delta^{18}\text{O}_{\text{IRMS}} = (1.007 \pm 0.019) \delta^{18}\text{O}_{\text{WVIA}} - (2.92 \pm 0.32)$ (solid lines), $R^2 > 0.99$.

Title Page

Abstract

Introduction

Conclusions

References

Tables

Figures

◀

▶

◀

▶

Back

Close

Full Screen / Esc

Printer-friendly Version

Interactive Discussion



Water vapor isotope measurements by OA-ICOS

P. Sturm and A. Knohl

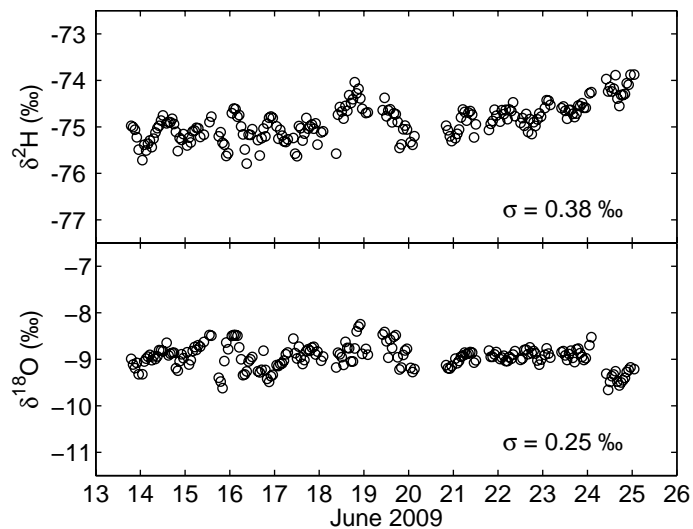


Fig. 10. Repeated analyses of a local water standard with our calibration system during 12 days. The standard deviation is 0.38‰ for $\delta^2\text{H}$ and 0.25‰ for $\delta^{18}\text{O}$, respectively.

[Title Page](#)[Abstract](#)[Introduction](#)[Conclusions](#)[References](#)[Tables](#)[Figures](#)[◀](#)[▶](#)[◀](#)[▶](#)[Back](#)[Close](#)[Full Screen / Esc](#)[Printer-friendly Version](#)[Interactive Discussion](#)